International Journal of Mechanics and Energy (IJME)
Vol. 4, Issue 2, 2016, ISSN: 2286-5845

Mixed Convection of Nanofluid Flows in a Ventilated Cavity Submitted to Varying Heating

Ismail Arroub[1], Ahmed Bahlaoui[1*], Abdelghani Raji[2], Mohammed Hasnaoui[3], Mohamed Naïmi[2]

[1] *Sultan Moulay Slimane University, Polydisciplinary Faculty, Interdisciplinary Laboratory of Research in Sciences and Technologies (LIRST), B. P. 592, Béni-Mellal 23000, Morocco.*

[2] *Sultan Moulay Slimane University, Faculty of Sciences and Technologies, Laboratory of Flows and Transfers Modelling (LAMET), B. P. 523, Béni-Mellal 23000, Morocco.*

[3] *Cadi Ayyad University, Faculty of Sciences Semlalia, Laboratory of Fluid Mechanics and Energetics (LMFE), B.P. 2390, Marrakech, Morocco.*

Abstract: The phenomenon of mixed convection heat transfer through Al_2O_3-water nanofluid inside a horizontal ventilated enclosure is studied numerically. The obtained results demonstrate clearly the positive role of the nanoparticles addition on the improvement of the heat transfer rate and the mean temperature within the cavity. The flow structure and the temperature distribution within the cavity are seen to be very affected by the Reynolds number and the heating type. Also, it is shown that, in general, the decreasing heating mode is more favorable to the heat transfer while the cooling efficiency is found to be more pronounced by applying the increasing heating type.

Key words: Mixed convection, ventilated cavity, injection, nanofluid, varying heating.

1. Introduction

The fluids that have been commonly used for heat transfer applications, such as water, ethylene glycol and oil, do not meet the rising demand as efficient heat transfer agents due to their inherently poor thermal conductivities. To overcome this problem, an innovative technique used to enhance heat transfer rates by adding nanoscale particles with low concentrations to the base fluid, has been extensively experimented. The resulting mixtures (nanofluids) have larger thermal conductivities than the base liquids which therefore leads to an increase of the heat transfer compared to that generated by the latter [1-3]. Since higher heat transfer rates are desirable in modern industrial applications, the mixed convection mechanism is recommended in problems involving nanofluids, where natural convection solely or forced convection solely are not able to provide effective cooling. Recently, mixed convection heat transfer in closed systems occurs by moving one (lid-driven) or two (double lid-driven) walls of the cavity confining the coolant fluid. Among the recently published works, we quote those by Karimipour et al. [4] and Goodarzi et al. [5] dealing with laminar and turbulent mixed convection heat transfer of Cu-water nanofluid in a rectangular lid-driven shallow enclosure heated from one side. It appears from these studies that the inclination angle of the cavity and the augmentation of the nanoparticles volume fraction could play a positive role in obtaining a better heat transfer. Mixed convection of nanofluids in ventilated cavities has been also the object of interest during the last years. Such problems are encountered in many industrial

* **Corresponding author:** Ahmed Bahlaoui
E-mail: bahlaoui75@yahoo.fr

applications such as heat exchangers, lubrication technology, chemical processing equipments, solar energy collectors and cooling of electronic equipment. In this perspective, Shahi et al. [6] conducted a numerical study of mixed convection flows of Cu-water nanofluid in a ventilated square cavity submitted to an imposed heat flux. The results presented indicate that the increase in solid concentration leads to an augmentation of the average Nusselt number at the heat source surface and, at the same time, to a decrease of the average bulk temperature. A similar problem was treated numerically by Mahmoudi et al. [7] with imposed temperature for different locations of inlet and outlet ports. The authors reported that, in the presence of nanoparticles, the bottom-top configuration was the most efficient compared to the remaining configurations considered in this study. In addition, the least effects accompanying the increase in solid concentration were observed in the case of top-top configuration. From their part, Sourtiji et al. [8] studied numerically mixed convection flows through an Alumina-water nanofluid in a square cavity with incoming oscillating flow for the top-bottom configuration. It is reported in this study that the increase of the volume fraction of nanoparticles engenders an improvement of heat transfer for all considered ranges of Strouhal and Richardson numbers. The same authors [9] considered the case where the incoming flow is steady and the inlet port is located on the upper part of the left wall whereas the location of the outlet port was varied along the four walls. It was observed that the performance of the nanoparticles on heat transfer enhancement is more pronounced at lower Richardson numbers.

It is clear that so far, the problem of nanofluid mixed convection within a ventilated cavity using the technics of injection or suction and submitted to non-uniform heating conditions has not been subject of any study yet. Therefore, the aim of the current study is to simulate numerically mixed convection heat transfer characteristics of water-based Al_2O_3 nanofluid flowing through a ventilated rectangular cavity. The consequence of varying the Reynolds number, $200 \leq Re \leq 5000$, the nanoparticle concentration, $0 \leq \phi \leq 0.1$, and the mode of heating (linearly increasing or decreasing temperature profile) on the dynamical and thermal characteristics of the flow and heat transfer performance have been investigated and discussed.

2. Problem Definition and Mathematical Modeling

The studied configuration is shown in Fig.1. It consists of a ventilated horizontal rectangular cavity of length L', height H' and having an aspect ratio A = 2. The cavity is heated from its bottom wall with a linearly increasing or decreasing temperature profile (Fig. 2) while the other boundaries are assumed to be adiabatic. The fluid in the enclosure is a water-based nanofluid containing Al_2O_3 nanoparticles. The physical system is subjected to an external flow which passes through the cavity by injection. The cold nanofluid enters the cavity from the bottom of the left vertical wall and leaves from the top of the right vertical one. The inlet and outlet ports have a constant dimensionless height, B = 1/4. Thus, it is assumed that both the base flow and nanoparticles are in thermal equilibrium and no slip occurs between them. The dispersed particles have a spherical shape and their size is assumed to be uniform. The properties of the nanofluid are assumed to be constant except for the density which is estimated by the Boussinesq approximation. The nanofluid is assumed Newtonian and incompressible. The flow is considered as laminar and two-dimensional. Therefore, using the following dimensionless variables:

$$A = L'/H' \;,\; B = h'/H' \;,\; x = x'/H' \;,\; y = y'/H' \;,$$

$$u = u'/u'_o \;,\; v = v'/u'_o \;,\; t = t'u'_o/H' \;,$$

$$T = (T' - T'_C)/(T'_H - T'_C),\; \Psi = \Psi'/u'_o H',\; \Omega = \Omega' H'/u'_o$$

$$Pr = \nu_f/\alpha_f\,,\quad Ra = g\,\beta_f (T'_H - T'_C)H'^3/\alpha_f \nu_f\,,\quad Re = u'_o H'/\nu_f$$

the corresponding set of differential equations using the vorticity-stream function (Ω-Ψ) formulation can be written in a dimensional form as follows:

$$\frac{\partial\Omega}{\partial t}+u\frac{\partial\Omega}{\partial x}+v\frac{\partial\Omega}{\partial y}=\frac{Ra}{Re^2 Pr}\left[\left(\frac{\varphi}{\left((1-\varphi)\frac{\rho_f}{\rho_s}+\varphi\right)}\right)\frac{\beta_s}{\beta_f}+\frac{1}{\left(\frac{\varphi}{(1-\varphi)}\frac{\rho_s}{\rho_f}+1\right)}\right]\frac{\partial T}{\partial x}$$
$$+\frac{1}{Re}\left[\frac{1}{(1-\varphi)^{2.5}\left(\varphi\frac{\rho_s}{\rho_f}+(1-\varphi)\right)}\right]\left(\frac{\partial^2\Omega}{\partial x^2}+\frac{\partial^2\Omega}{\partial y^2}\right) \tag{1}$$

$$\frac{\partial T}{\partial t}+u\frac{\partial T}{\partial x}+v\frac{\partial T}{\partial y}=\frac{1}{Re\,Pr}\left(\frac{\frac{\lambda_{nf}}{\lambda_f}}{(1-\varphi)+\varphi\frac{(\rho c_p)_s}{(\rho c_p)_f}}\right)\left(\frac{\partial^2 T}{\partial x^2}+\frac{\partial^2 T}{\partial y^2}\right) \tag{2}$$

$$\frac{\partial^2\Psi}{\partial x^2}+\frac{\partial^2\Psi}{\partial y^2}=-\Omega \tag{3}$$

The dimensionless horizontal and vertical velocities are converted to:

$$u=\frac{\partial\Psi}{\partial y}\quad;\quad v=-\frac{\partial\Psi}{\partial x}\quad \text{and}\quad \Omega=\frac{\partial v}{\partial x}-\frac{\partial u}{\partial y} \tag{4}$$

The nanofluid effective density, effective thermal conductivity, thermal diffusivity, heat capacitance and the thermal expansion coefficient of the nanofluid are, respectively, given by:

$$\rho_{nf}=\phi\rho_s+(1-\phi)\rho_f \tag{5}$$

$$\frac{\lambda_{nf}}{\lambda_f}=\frac{\lambda_s+2\lambda_f-2\phi(\lambda_f-\lambda_s)}{\lambda_s+2\lambda_f+\phi(\lambda_f-\lambda_s)} \tag{6}$$

$$\alpha_{nf}=\frac{\lambda_{nf}}{(\rho c_p)_{nf}} \tag{7}$$

$$(\rho c_p)_{nf}=\phi(\rho c_p)_s+(1-\phi)(\rho c_p)_f \tag{8}$$

$$(\rho\beta)_{nf}=\phi\rho_s\,\beta_s+(1-\phi)\rho_f\beta_f \tag{9}$$

Where *"f"*, *"s"* and *"nf"* indicate fluid, solid particles and nanofluid respectively.

2.1 Boundary Conditions

The boundary conditions applied to the problem are written as:

$u = v = 0$ on the rigid walls

$T=(-\frac{2a}{A})\,x+(1+a)$ on the lower horizontal heated wall

$\frac{\partial T}{\partial n}=0$ on the adiabatic walls

$\Psi = 0$ on the walls below the two openings

$\Psi = B$ on the walls above the two openings

$T = 0$, $\Psi = y$, $\Omega = 0$, $u = 1$, $v = 0$ at the inlet port

- The boundary conditions are unknown at the outlet opening. Values of u, v, T, Ψ and Ω are extrapolated at each time step by considering zero second derivatives of these variables at the exit of the cavity.
- a = 0.5/(-0.5) for decreasing/(increasing) heating temperature profile.
- *"n"* indicates the normal direction to the considered adiabatic wall.

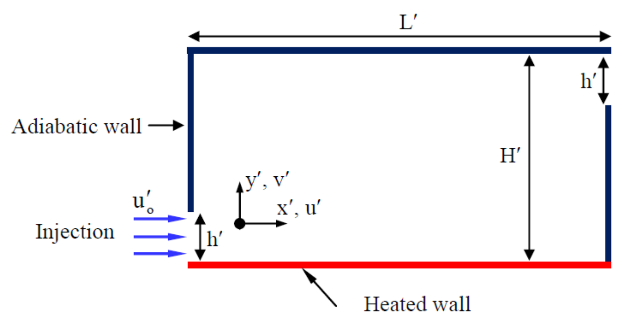

Fig. 1 : Sketch of the geometry and coordinates system

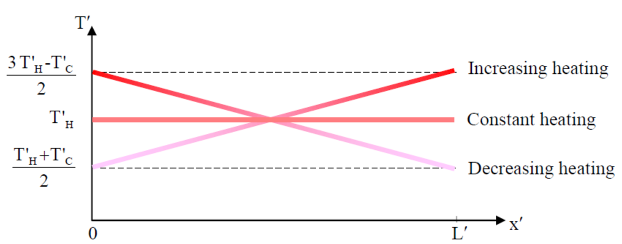

Fig. 2 : Imposed temperature profiles on the heated wall

2.2 Heat Transfer

The estimation of the heat transfer enhancement and efficient cooling is done based on the average Nusselt number, *Nu*, calculated on the heated bottom wall of the cavity such as:

$$Nu = -\frac{1}{A}\left(\frac{\lambda_{nf}}{\lambda_f}\right)\int_0^A \frac{\partial T}{\partial y}\bigg|_{y=0} dx \qquad (10)$$

3. Numerical Approach

The numerical algorithm used to solve the dimensionless governing equations, (1)-(3), is based on the finite difference technique. The second-order upwind approach is used to discretize the advection terms to avoid possible instabilities frequently encountered in mixed convection problems. Also, the second order central difference scheme is adopted to approximate the first and second derivatives of the diffusive terms. Thereafter, the integration of the vorticity and energy equations, (1) and (2), is performed iteratively with the alternating direction implicit (*ADI*) method. To satisfy the mass conservation, the Poisson equation, (3), is solved by a point successive over-relaxation method (*PSOR*) with an optimum over-relaxation factor equal to 1.95 for the grid (201×101) retained in this work.

4. Results and Discussion

In this section, the Rayleigh number was kept at a constant value $Ra = 10^6$ and the Reynolds number *Re* ranging between 200 and 5000. Values of these parameters involves values of the Richardson number, $Ri = Ra / Re^2\, Pr$, varying in the range [6.45×10^{-3}, 4.03] which simulates natural convection, mixed convection and forced convection dominating regimes. In the following, effects of nanofluids and modes of heating on flow pattern and thermal structure and on efficient cooling are investigated. Before dealing with this part of the results, it is to note that in the case of an increasing heating temperature profile, the flow is unsteady as *Re* is very weak. Therefore, the dynamical and thermal structures could not be presented in this situation.

Streamlines and isotherms plots illustrating the effect of *Re* on the dynamical and thermal fields, in the increasing heating mode, are shown in Figs. 3a-3d for both $\phi = 0$ (solid line —) and $\phi = 0.1$ (dashed line - - -). For a moderate value of *Re* (*Re* = 800), the streamlines show the presence of two closed convective cells separated by the open lines of the forced flow (Fig. 3a). More precisely, a big trigonometric cell, due to shear effect, is positioned in the upper part of the cavity while the small clockwise one, due to free convection and shear effect is located below the open lines. However, no changes have been noted about flow structures by passing from $\phi = 0$ to $\phi = 0.1$, except the small cell whose size varies relatively. The corresponding isotherms, at the level of the heated horizontal wall, are progressively tightened from the inlet indicating a good convective heat exchange between the heating surface and the nanofluid in accordance with the imposed increasing temperature profile. Also, half of the cavity beyond the developed thermal boundary layer is at a uniform cold temperature. This aspect testifies of the absence of thermal interaction between the active wall and the left and top walls through the forced flow. In addition, the isotherms for nanofluid ($\phi = 0.1$) are not consistent with the case of pure fluid ($\phi = 0$) at the right of the bottom wall. They are well stratified and dispersed along the thermal boundary layer. This is explained by a good heat exchange between the hot wall and the open lines through the small cell and also a good homogenization of the temperature within the cavity by considering nanofluid. More increase of *Re* up to 1000 leads to an increase of the size and intensity of the lower cell as a result of the increase of the effect of forced convection (Fig. 3b). A further increase of *Re* up to 3000 and 5000 successively (dominant forced convection regime), as shown in Figs. 3c-3d, promotes lower cell, in terms of size, to the detriment of the space allowed in the lower part of the cavity, while the upper cell is divided into two others ones due to the large shear effect resulting from the growing forced convection. Furthermore, the shape of the flow is characterized by open parallel straight lines joining the two openings. The corresponding isotherms illustrate that all isotherms are condensed near the hot wall, which justifies that the heat provided by the isothermal wall is carried by the forced flow to the outlet without passing through the remainder space of the cavity. Also, as expected, thermal and dynamical structures become insensitive to the nanoparticles concentration for large values of *Re*.

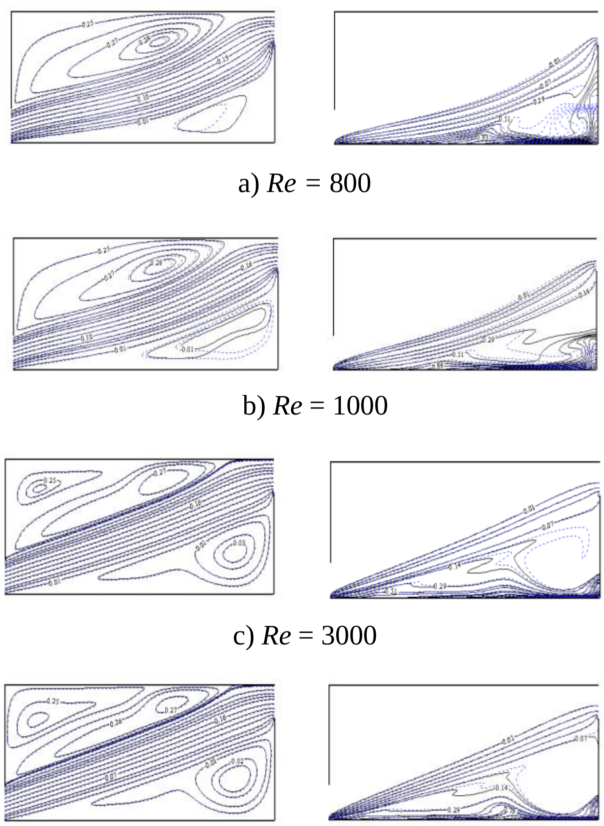

a) *Re* = 800

b) *Re* = 1000

c) *Re* = 3000

d) *Re* = 5000

Fig.3 : Streamlines and isotherms, in the increasing heating mode, for $\phi = 0$ (—) and $\phi = 0.1$ (- - -) at different values of *Re*: a) *Re* = 800, b) *Re* = 1000, c) *Re* = 3000 and d) *Re* = 5000.

Comparisons of the streamlines and isotherms contours between pure water ($\phi = 0$) and nanofluid ($\phi = 0.1$), in the decreasing heating temperature profile, are also displayed in Figs. 4a-4d, for various values of *Re*. According to the Fig. 4a, the streamlines obtained for low values of *Re* (*Re* = 200) show the presence of one big trigonometric cell, due to the shear effect, surmounting the open lines of the forced flow. The corresponding isotherms are very dense on the hot wall near the entrance. This behavior is explained by the decreasing profile of the hot wall temperature. This suggests that the released heat towards the forced flow is predominantly occurs through the left half of the heated wall. As seen, the thickness of the thermal boundary layer grows to the outlet opening because of the assisting effects of forced and free convection flows. The remaining part of the cavity is considered as a thermally inactive area. More increase of *Re* to 1000 (Fig. 4b) contributes to the development of the lower secondary cell in size and intensity. This effect accentuated by forced convection contributes likewise to the increase of the thermal boundary layer so that this latter represents almost the lower triangular area of the cavity. By increasing progressively *Re* to 3000 and 5000, as illustrated respectively in Figs. 4c-4d, it is found that the dominating heat transfer mechanism changes to the forced one and the flow crosses the cavity diametrically between the two openings without being significantly affected by the lower closed cell. It appears important to note that through all these values of *Re*, the flow patterns do not change significantly when the solid volume fraction of the nanofluid is equal to $\phi = 0.1$ when compared with the pure fluid (water). However, the addition of 10 % of nanoparticles to the base fluid affects clearly the temperatures distribution since $Re \leq 1000$. Indeed, the presence of solid particles homogenizes relatively the temperature within the cavity what contributes to the reduction of the cold zone.

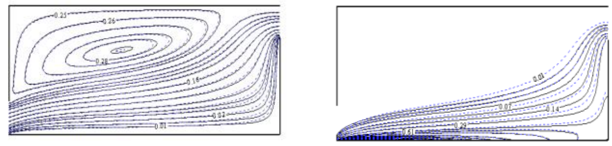

a) Re = 200

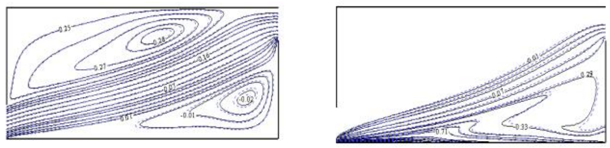

b) Re = 1000

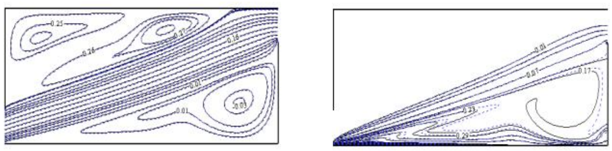

c) Re = 3000

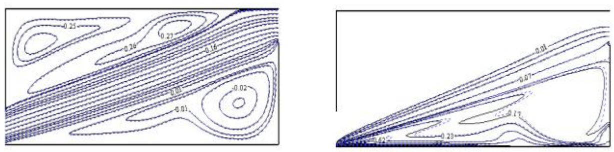

d) Re = 5000

Fig.4 : Streamlines and isotherms, in the decreasing heating mode, for $\phi = 0$ (—) and $\phi = 0.1$ (- - -) at different values of *Re*: a) *Re* = 200, b) *Re* = 1000, c) *Re* = 3000 and d) *Re* = 5000.

In order to illustrate the performance of the injection mode in the heat removal, variations versus the Reynolds number of the average Nusselt number, Nu, along the heated wall are presented in Fig. 5 for the two heating temperature profiles and different values of ϕ. For a decreasing heating temperature profile, a monotonous increase of Nu with Re is generally observed. The rate of this increase becomes more important from $Re \approx 500$ (an increase in the slope of the curves is observed from this threshold). This tendency is justified by the flow intensification promoted by the increase of Re. In the increasing heating case, it can be noted that the increase of Nu with Re remains very limited as long as $Re \leq 500$. Then, a slight decrease of Nu with Re is observed up to a critical value, $Re_{CR} \approx 1000$. The decrease of the mixed convection effect, occurring in the transition phase toward the forced flow regime, is attributed to the appearance of the closed cell between the right end of the hot wall, where heating is greatest, and the open lines and consequently the delaying of heat released by the hot wall towards outside through the open lines. Beyond this threshold value of Re, the tendency is reversed; the evolution of Nu is then characterized by a monotonic increase with Re resulting from an enhanced thermal interaction between the heated wall and the dominant forced flow. For a fixed value of Re, the increase of the solid volume fraction ϕ up to 0.1 leads to a noticeable growing effect of the convection either for increasing or decreasing heating case. This is due to the increase in effective thermal conductivity of the nanofluid with the increase in ϕ. But, it is reported that this effect is weaker in the increasing mode when natural convection is predominated. More precisely, by increasing ϕ from 0 to 0.1, Nu is increased, for the more favorable case obtained for Re = 5000, from 27.22/(31.04) to 31.77/(36.88) for the increasing/decreasing temperature profile respectively. It should be noted that the decreasing heating enhances more the heat transfer in comparison with the increasing heating for moderate and high values of Re, either in case of a cavity filled with pure fluid (water) or with nanofluid. This result permits a better heat removal from the hot wall by applying the decreasing heating. Quantitatively, for most important case (Re = 1500 and ϕ = 0.1), passing from the increasing mode to the decreasing one, Nu increases from 17.28 to 23.88 which corresponds to an enhancement of the heat transfer by about 38.19 %. However, for natural convection dominating regime (weak values of Re), the heating mode effect is reversed and the thermal efficiency, expressed in terms of released heat, is relatively favored by the increasing heating.

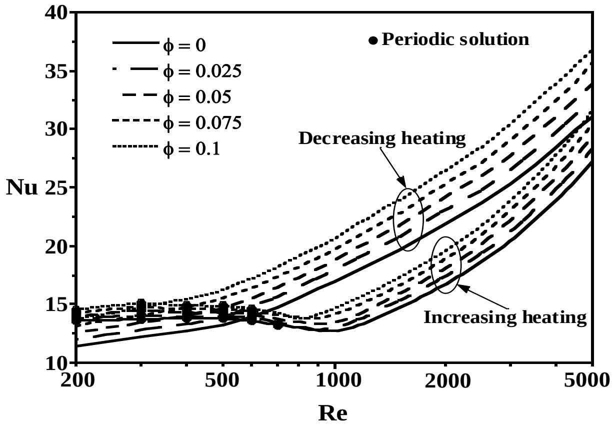

Fig. 5: Variations, with *Re*, of the average Nusselt number, *Nu*, for different values of ϕ in both increasing and decreasing heating cases.

For practical reasons, the evaluation of mean temperature of the fluid inside the cavity is of a great importance. Thus, variations of this parameter with *Re* are plotted in Fig. 6 for both increasing and decreasing heating temperature profiles and different values of ϕ. As clearly seen in both cases of heating, the average temperature $\overline{T}$ increases by increasing *Re* up to a critical value ranging in [600-900] which strongly depends on ϕ and the heating temperature profile. This reheating of the cavity is justified by the growing combined effect of forced and natural convections resulting from their assisting flows. Then, this tendency is reversed whatever the heating mode because the growing of *Re* is marked by a decrease of $\overline{T}$; this behavior is due to the forced convection predominant effect which drives out the heat towards the outside and thereafter contributes to the cooling of the cavity. For a given value of *Re*, it is qualitatively shown that when solid concentration increases, the average temperature increases, for the two heating modes, because the presence of nanoparticles leads to a good heat exchange by convection in the cavity and contributes consequently to an increase of the average temperature. Also, it is obvious from this figure that the increasing heating mode leads generally to a better cooling of the cavity since the resulting values of $\overline{T}$ are lower in comparison with the decreasing heating. Except for the short predominance area of the mixed convection corresponding to $700 \le Re \le 1000$ for which decreasing heating presents the most cooling efficiency. For reasons of clarity, it is noted that, for ϕ = 0.1 and *Re* = 2000, a reduction of about 15% of $\overline{T}$ occurs when passing from the decreasing heating temperature profile to the increasing one.

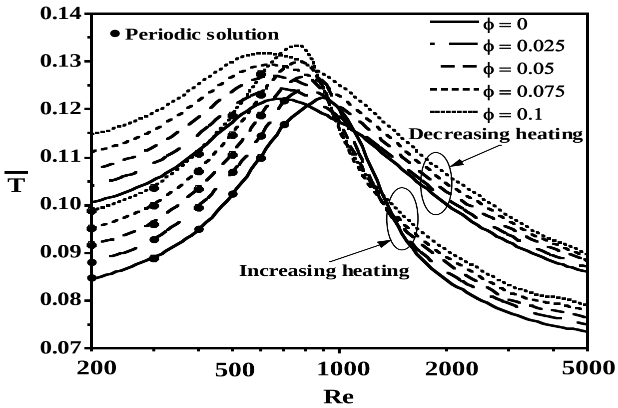

Fig. 6: Variations, with *Re*, of the mean temperature, $\overline{T}$, for different values of ϕ in both increasing and decreasing heating cases.

5. Concluding remarks

A numerical analysis has been performed to study the laminar two-dimensional mixed convection flow of Al_2O_3-water nanofluid in a horizontal ventilated enclosure heated from below and cooled by an external flow. The study is carried out by considering two types of heating (linearly increasing and decreasing heating). From the study, it has been found that the flow and temperature profiles are affected depending on the mode of applied heating. Also, the results illustrate that the suspended nanoparticles substantially increase the heat transfer rate through the cavity and the average temperature within the enclosure by applying both increasing and decreasing heating modes. On the other hand, it is to remember that the decreasing heating mode gives a better thermal efficiency than the increasing heating mode by leading to more heat transfer across the cavity even with or without the presence of nanoparticles. However, this trend is reversed for natural convection predominance (low values of *Re*) when the thermal removal is relatively favored by the increasing heating. In addition, it is found that a better cooling of the cavity is generally reached by applying the increasing heating (for low and high values of *Re*) since these cases lead to lower values of the mean temperature.

References

[1] S.E.B. Maïga, S.J. Palm, C.T. Nguyen, G. Roy, N. Galanis, Heat transfer enhancement by using nanofluids in forced convection flows, Int. J. Heat Fluid Flow, 26(4), (2005), 530-546.

[2] Y. He, Y. Jin, H. Chen, Y. Ding, D. Cang, H. Lu, Heat transfer and flow behaviour of aqueous suspensions of TiO_2 nanoparticles (nanofluids) flowing upward through a vertical pipe, Int. J. Heat Mass Transfer, 50, (2007), 2272-2281.

[3] R. Nasrin, M.A. Alim, A.J. Chamkha, Buoyancy-driven heat transfer of water-Al_2O_3 nanofluid in a closed chamber: Effects of solid volume fraction, Prandtl number and aspect ratio, Int. J. Heat Mass Transfer, 55, (2012), 7355-7365.

[4] A. Karimipour, M.H. Esfe, M.R. Safaei, D.T. Semiromi, S. Jafari, S.N. Kazi, Mixed convection of copper-water nanofluid in a shallow inclined lid driven cavity using the Lattice Boltzmann method, Physica A, 402, (2014), 150-168.

[5] M. Goodarzi, M.R. Safaei, K. Vafai, G. Ahmadi, M. Dahari, S.N. Kazi, N. Jomhari, Investigation of nanofluid mixed convection in a shallow cavity using a two-phase mixture model, Int. J. Therm. Sci., 75, (2014), 204-220.

[6] M. Shahi, A.H. Mahmoudi, F. Talebi, Numerical study of mixed convective cooling in a square cavity ventilated and partially heated from the below utilizing nanofluid, Int. Comm. Heat Mass Transfer, 37(2), (2010), 201-213.

[7] A.H. Mahmoudi, M. Shahi, F. Talebi, Effect of inlet and outlet location on the mixed convective cooling inside the ventilated cavity subjected to an external nanofluid, Int. Comm. Heat Mass Transfer, 37(8), (2010), 1158-1173.

[8] E. Sourtiji, S.F. Hosseinizadeh, M. Gorji-Bandpy, D.D. Ganji, Effect of water-based Al_2O_3 nanofluids on heat transfer and pressure drop in periodic mixed convection inside a square ventilated cavity, Int. Comm. Heat Mass Transfer, 38(8), (2011), 1125-1134.

[9] E. Sourtiji, M. Gorji-Bandpy, D.D. Ganji, S.F. Hosseinizadeh, Numerical analysis of mixed convection heat transfer of Al_2O_3-water nanofluid in a ventilated cavity considering different positions of the outlet port, Powder Technology, 262, (2014), 71-81.